

Electronic structure of the carbon vacancy in NbC

W. E. Pickett and B. M. Klein

Condensed Matter Physics Branch, Naval Research Laboratory, Washington, D.C. 20375-5000

R. Zeller

Institut für Festkörperforschung der Kernforschungsanlage Jülich, Postfach 19 13, D-5170 Jülich, Federal Republic of Germany

(Received 3 March 1986)

The electronic structure of an isolated carbon vacancy in the $B1$ -structure NbC is studied with use of the muffin-tin Green's-function method. Both the vacancy region and the neighboring shell of Nb atoms are allowed to readjust self-consistently to the absence of the carbon atom. The change in the electronic density of states is dominated by a Γ_1 (s -like) symmetry vacancy-induced peak 2.6 eV below the Fermi level E_F arising from a symmetric combination of surrounding Nb d states. A smaller, broader Γ_{15} symmetry peak, also composed of Nb states, occurs around 1.75 eV below E_F . The present results suggest that the peak at 1.9 eV below E_F seen in the x-ray photoemission spectrum of NbC_{0.85} by Höchst *et al.*, although semiquantitatively well described by the present results, is significantly influenced by vacancy-vacancy interactions and/or short-range ordering of vacancies.

I. INTRODUCTION

The carbides and nitrides of group-IVB and -VB transition metals possess extraordinary properties,¹ including extreme hardness, high melting temperatures approaching 4000 K, and a wide range of superconducting transition temperatures. This class of materials also displays widespread substoichiometry, primarily on the nonmetal sublattice, with vacancy concentrations as high as 50 at. % at or near thermal equilibrium. Nevertheless, the rocksalt ($B1$) phase remains the stable one over a wide range of compositions. Unfortunately, the high vacancy concentration is detrimental to many desirable properties. An example is the superconducting transition temperature, T_c , in NbC, which is relatively high ($T_c \simeq 11$ K) near stoichiometry but falls to zero² for 20% vacancies on the carbon sublattice.

The proclivity of the class of transition-metal carbonitrides to substoichiometry on the nonmetal sublattice seems to be a fundamental "property" of these carbonitrides. Huisman *et al.*³ have even found indications from model electronic structure calculations that the nonmetal vacancy formation energy is *positive* in TiC, but *negative* in TiO, consistent with the experimental situation in these compounds. The more typical case is that, although vacancies raise the energy of the system, finite vacancy concentrations are stabilized at nonzero temperature by the accompanying increase in entropy. In such a case the vacancy formation energy is the limiting factor rather than the driving force. From the viewpoint of first-principles studies it is simpler, both conceptually and computationally, to deal with a single vacancy in an otherwise perfect crystal rather than to treat a finite concentration of randomly positioned vacancies. In fact, this simplification from the finite vacancy concentration to the isolated vacancy may be important in understanding the underlying driving force for substoichiometry.

In this paper we concern ourselves with the electronic structure of the C vacancy in NbC. This system was first addressed theoretically by Schwarz and Röscher⁴ using cluster models with and without a carbon atom at the center. From self-consistent $X\alpha$ scattered wave calculations on 27 atom clusters these authors found a vacancy related density of states (DOS) peak of p -like symmetry about 1.4 eV below the Fermi level E_F . Ries and Winter⁵ extended the self-consistency to 53 atom clusters and, in addition, they mimicked ideal crystal conditions by assigning bulk Nb and C potentials to atoms near the surface of the cluster rather than allowing them to adjust to the presence of the surface. This *ad hoc* hybrid procedure resulted in a DOS peak of s symmetry 2.7 eV below E_F .

The experimental evidence on the electronic structure of the C vacancy rests on the x-ray photoelectron spectroscopy (XPS) of Höchst *et al.*⁶ Subtracting the spectrum of photoelectrons of NbC_{0.96} from that of NbC_{0.85} they obtained a difference spectrum which has a peak 1.9 eV below E_F but is featureless otherwise. Taking into account the stated spectrometer resolution we estimate the intrinsic width of this peak (FWHM) to be 0.6–0.7 eV. There is no experimental information on the symmetry of the states in this peak.

Since the data of Höchst *et al.* were taken on samples with rather high concentration of vacancies, it may be more relevant (unless vacancy ordering occurs) to compare with the DOS spectra of coherent-potential approximation (CPA) "alloy" calculations on NbC _{x} than with the single-impurity-cluster calculations. Three such calculations have been reported. Klima⁷ and Klein *et al.*⁸ found no structure in the region of several eV below E_F while Pecheur *et al.*⁹ obtained a peak of p symmetry 1.5 eV below E_F . Unfortunately each of these calculations relies on empirically determined parameters and assumptions about the representation of the vacancy, and it has become clear that the results are sensitive to the choice of param-

Work of the U. S. Government
Not subject to U. S. copyright

ters pertaining to the vacant site.

Due to the importance of having a clear understanding of the isolated vacancy and the confusion arising from previous investigations, we have applied the self-consistent muffin-tin Green's function method to determine the electronic structure of the C vacancy in NbC. The method is discussed briefly in Sec. II. A discussion of the results is given in Sec. III and the implications for the properties of carbides are presented in Sec. IV.

II. METHOD OF CALCULATION

The calculations are based on density-functional theory¹⁰ in the local-density approximation.¹¹ The one-electron potential is treated in the same muffin-tin approximation which has been used in previous studies^{8,12} of NbC. For the defect problem the Green's function G is of central interest. For a collection of nonoverlapping muffin-tin potentials $v_n(|\mathbf{r}-\mathbf{R}^n|)$ centered at positions \mathbf{R}^n , G can be expanded into eigensolutions of the local muffin-tin potentials in the form

$$\begin{aligned} G(\mathbf{r}+\mathbf{R}^n, \mathbf{r}'+\mathbf{R}^{n'}; E) \\ = G_s(\mathbf{r}+\mathbf{R}^n, \mathbf{r}'+\mathbf{R}^{n'}; E)\delta_{nn'} \\ + \sum_{L, L'} Y_L(r) R_L^n(r, E) G_{LL'}^{nn'}(E) R_L^{n'}(r', E) Y_{L'}(r'). \end{aligned} \quad (1)$$

In Eq. (1) $L=(l, m)$ is the angular momentum index, Y_L are the spherical harmonics and $R_L^n(r, E)$ are the regular solutions of the radial Schrödinger equation for the spherical potential $v_n(r)$ and energy E . G_s is the Green's function for a single muffin-tin potential v_n in free space.¹³

Multiple scattering of the electron between muffin tins is described by the structural Green's function $G_{LL'}^{nn'}$. It can be related to its counterpart $G_{LL'}^{0nn'}$ for the perfect crystal by the Dyson equation

$$G_{LL'}^{nn'}(E) = G_{LL'}^{0nn'}(E) + \sum_{n'', L''} G_{LL''}^{0nn''}(E) \Delta t_{L''}^{n''}(E) G_{L''L'}^{n''n'}(E). \quad (2)$$

In this equation $\Delta t_{L'}^n = t_{L'}^n - t_{L'}^{0n}$ is the difference between the t matrices of the disturbed system and the ideal crystal.

The numerical techniques used in the solution of Eq. (2) have been described in detail previously,¹⁴ so only information relevant to current calculations will be presented here. The host crystal Green's function was constructed from bands up to energies 10 eV above the Fermi level. The necessary Brillouin zone integrations were performed by the tetrahedron method using 324 points in the irreducible zone. The bands were obtained using the augmented-plane-wave method using a lattice constant of $a = 4.4685 \text{ \AA} = 8.4471 \text{ a.u.}$ and muffin-tin radii $R_{\text{MT}}(\text{Nb}) = 2.3235 \text{ a.u.}$ and $R_{\text{MT}}(\text{C}) = 1.900 \text{ a.u.}$ The angular momentum expansion in $G_{LL'}^{nn'}$ and $G_{LL'}^{0nn'}$ includes s , p , and d electrons.

In the current calculation of the carbon vacancy the potentials on vacant site and on the Nb atoms neighboring the vacancy are allowed to respond self-consistently to the vacancy. Beyond this shell of neighbors the perturbation of the host is neglected. The resulting 63×63 matrix Eq. (2) is symmetrized as described previously,¹⁴ resulting in

several smaller matrix equations to be solved. The vacancy and Nb potentials and charge densities are determined self-consistently. The necessary charge density is obtained by complex energy integration up to the Fermi energy of the host using 32 complex energies.¹⁵

III. NUMERICAL RESULTS

The local density of states (LDOS) inside the vacant Wigner-Seitz sphere is shown in Fig. 1, as is the LDOS for host C atom. The primary feature is a strong s -like peak of width 0.5 eV (FWHM) centered 2.6 eV below E_F . Also shown in Fig. 1 is the l decomposition of the LDOS inside the vacancy sphere. For p -symmetry states there is a small peak centered at -1.75 eV (all energies will be given relative to E_F) on top of a smooth broad background. This small p -like peak falls at the minimum in the host DOS and reflects the tendency of defects to broaden the DOS, which washes out peaks and fills in "valleys" in the DOS.

The LDOS on the Nb atom adjacent to the vacancy is shown in Fig. 2, together with the *change* of LDOS (defect system minus host) decomposed into s , p , and d contributions. The strong vacancy related peak at -2.6 eV is seen to extend to the Nb site, where it is primarily d like with a small ($\sim 15\%$) p contribution. Figure 2 indicates that the secondary peak at -1.75 eV is strongly associated with the Nb site where it is entirely of d character. At other energies the effect of the vacancy is to shift states out of peaks and into valleys, and to move all structure upward slightly reflecting a *repulsive effect* of the vacancy on the Nb potential.

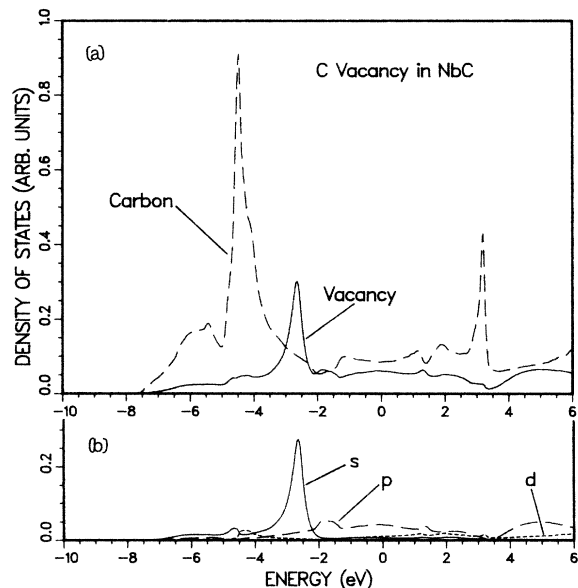


FIG. 1. (a) Local density of states of the carbon vacancy (solid line) compared to that of the host carbon atom (dashed line). (b) Decomposition of the vacancy density of states into s , p , and d components (solid, dashed, and dotted lines, respectively).

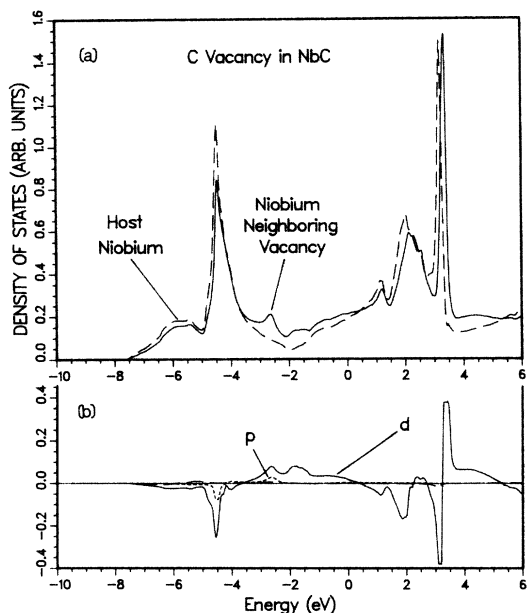


FIG. 2. (a) Local density of states of a Nb atom neighboring the vacancy (solid line) and of a host Nb atom (dashed line). (b) The Nb difference density of states (defect minus host) decomposed into p and d components (dotted, and solid lines, respectively). The s difference is negligible on this scale.

The vacancy potential, shown in Fig. 3 in comparison to the host carbon potential, is repulsive, so it will not bind any atomlike states. Since the interesting LDOS structure lies in a region of Nb d states, the “vacancy-related” structures reflect the effects of the vacancy on the Nb d states. In NbC the Nb e_g orbitals form strong

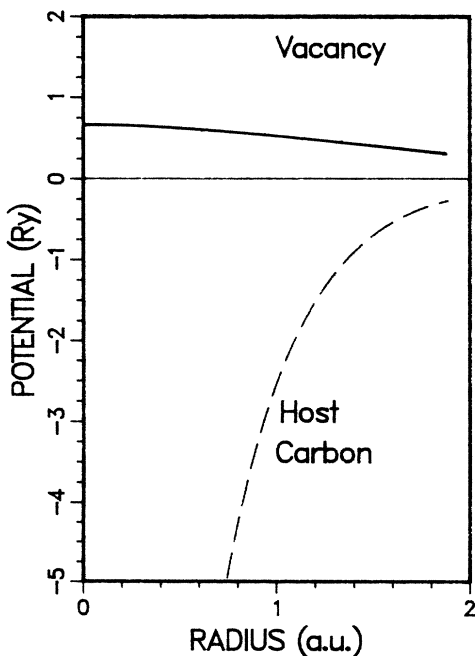


FIG. 3. Comparison of the vacancy potential (solid line) and the host carbon potential (dashed line). The sphere radius is 1.9025 a.u.

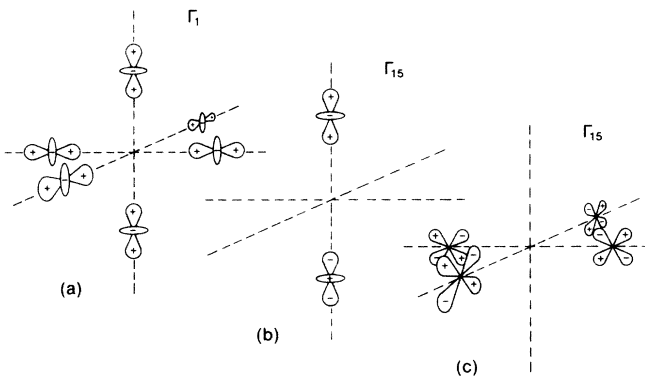


FIG. 4. Schematic indication of the linear combinations of d functions on Nb atom surrounding the vacancy which form high-symmetry representations of the vacancy point group.

($pd\sigma$) bonds with the C p orbitals, corresponding to the strong peak in the host density of states at -4.5 eV. In Fig. 4 we indicate the linear combinations of d states on the Nb shell of atoms which have the highest symmetries with respect to the vacant site. (Pecher *et al.*⁹ have provided all of the representations of the vacancy point group for this problem.) Figure 4(a) indicates the fully symmetric combination of $d(e_g)$ states of Γ_1 symmetry. The absence of the carbon atom eliminates the ($pd\sigma$) bonding and the repulsive vacancy potential (Fig. 3) pushes the Γ_1 combination of e_g states upward forming the peak at -2.6 eV.

Figures 4(b) and 4(c) each show one member of the two distinct Γ_{15} (p -like) symmetry combinations of d states on the Nb shell, formed from two $d_{3z^2-r^2}$ and from four d_{xz} , d_{yz} functions, respectively. These combinations form the secondary peak in the vacancy DOS at -1.75 eV.

The partial charges within the respective Wigner-Seitz spheres [$R_{WS}(\text{Nb})=2.854$ a.u., $R_{WS}(\text{C})=2.334$ a.u.] are given in Table I. As expected, the s and p charge in the vacant sphere decreases sharply, reflecting the removal of the four carbon sp valence electrons. The valence charge within the sphere decreases by only 3.54 electrons (the host had 4.67 C electrons), reflecting the spilling of host charge into the vacancy. Each neighboring Nb atom loses 0.05 electrons (0.01 s , 0.04 p) to the charge in the vacancy, making 0.30 electrons contributed from the Nb shell. The remaining 0.16 electrons flow in from further shells.

TABLE I. The partial valence charges within the carbon and niobium spheres for the host and for the vacancy defect system. Q_{net} gives the net charge within the sphere, equal to the atomic number minus the electronic charge (taking into account core charges). Values are rounded to the nearest 0.01 electron.

	C site		Nb site	
	Host	Defect	Host	Defect
s	1.44	0.64	0.41	0.40
p	3.06	0.38	0.70	0.66
d	0.18	0.12	3.22	3.22
Total	4.67	1.13	4.33	4.28
Q_{net}	-0.67	-1.13	+0.67	+0.72

IV. DISCUSSION

Of the previous calculations mentioned in the Introduction, those of Ries and Winter⁵ alone give results similar to ours. Using 53 atom clusters these authors obtained a sharp peak of Γ_1 symmetry about 2.7 eV below E_F . This feature, at an energy which is essentially identical to ours, was obtained in spite of differences in shape of the host density of states between their cluster calculation and our crystalline band structure calculation. They also obtained secondary peaks in the vacancy p DOS at -2.7 eV (same energy as the s peak) and at E_F , as compared with our single feature at -1.75 eV. Nevertheless the most important feature is faithfully described by their cluster calculation.

Earlier cluster calculations by Schwarz and Röscher⁴ using 27 atom clusters resulted in a p -like vacancy state lying about 1.4 eV below E_F . This incorrect result apparently reflects the sensitivity of individual states to cluster size when the number of atoms in the cluster is too small. Although *well localized* defect states, such as might occur for substitutional impurities, may be modeled reasonably by rather small clusters, the vacancy state in the present calculation is not so strongly localized and seems to be particularly sensitive to cluster size. Cluster size will also be more important in compounds which, like NbC, have some ionic character. Ries and Winter compensated for this effect by *assigning* bulk potentials to the Nb and C atoms in the outer shells rather than allowing them to respond to the cluster surface.

Pecheur, Toussaint, and Kauffer⁹ performed empirical tight-binding calculations of the LDOS (in integrated form) of the C vacancy. They extend the previously used description of the vacancy by a diagonal, infinite potential on the vacancy site by additional terms to account for changes on the nearest Nb neighbors and to satisfy the Friedel sum rule. For their choice of potential and for their method of calculation they concluded that the change in the s -like density of states below E_F due to the vacancy is unimportant, and they obtained only a p -like peak at -1.5 eV. Their choice of parameters appears to have been influenced by the experimental photoemission peak (see below). For the vacancy s DOS they obtained structure 4–6 eV above E_F which is absent in our calculation (Fig. 1).

Morinaga *et al.*¹⁶ have applied the scattered wave $X\alpha$ method to model nonmetal vacancies in NbO, NbN, and NbC. While their ionic model of 18 atom clusters showed clear vacancy related states below E_F for NbO, these states were hardly discernible in NbC. These results again reflect the inability of small clusters to model solid state effects accurately.

The only direct experimental information on the electronic structure of the C vacancy is from the x-ray photoemission spectra (XPS) of Höchst *et al.*,⁶ taken on NbC_{0.96} and NbC_{0.85}. The difference spectra reveals a peak at -1.9 eV in the $x=0.85$ sample which is not present in the more nearly stoichiometric material. No information on the symmetry of the states in this peak is available. Naturally this experimental peak has been interpreted as vacancy induced states. It is worth noting

that no corresponding peak is visible in the ultraviolet photoemission spectroscopy data of Weaver and Schmidt¹⁷ on NbC_{0.92}. The intrinsic width of the XPS peak (after accounting for the spectrometer resolution) of 0.6–0.7 eV is only slightly larger than the width of our calculated peak (~ 0.5 eV).

There is a 0.7 eV discrepancy between the position of our calculated peak for an isolated C vacancy and the experimental data obtained for 15 at. % C vacancies. On the experimental side, it is clear that for such a large concentration of vacancies the interaction of vacancies is not negligible. In the $B1$ structure a C atom has 12 C neighbors on the fcc nonmetal sublattice. For 15% vacancies, then, a vacancy will be surrounded on the average by ten carbon atoms and two vacancies on the carbon sublattice. For such a situation almost every Nb atom may neighbor a vacancy and many may be neighbor to two vacancies and, thus, there will be no Nb atoms (nor C atoms) which are characteristic of the bulk. Therefore, it would be highly desirable to have high-resolution XPS data on samples with 5% or less carbon vacancies to compare with our calculations.

There is another reason why the peak in the XPS data for NbC_{0.85} may not be representative of the isolated vacancy. It is known that for NbC _{x} samples near the integral composition Nb₆C₅, as this one is, there is strong tendency toward vacancy ordering,^{18–26} i.e., formation of the ordered compound. In the ordered material the periodic array of vacancies can give rise to strongly vacancy related Bloch bands whose spectral weight is shifted by the periodic potential. Even if the ordering is only partial or short range a remnant of this effect may remain.

Of course our calculations are not entirely representative of the true isolated C vacancy in NbC. As mentioned above we have neglected *changes* in potential (and implicitly the density) beyond the first shell of Nb atoms. However, preliminary single-site calculations in which the neighboring Nb potentials were not allowed to readjust give similar results (the s peak occurs at -3.0 eV rather than -2.6 eV). This small difference, and the metallic screening of the defect potential, leads us to believe that extending the self-consistency to further shells would not alter the position of the DOS peak appreciably. Other calculational restrictions, such as the frozen core approximation and neglect of $l \geq 3$ components of the density around the atoms, also are not expected to be serious limitations.

Another feature which we have not included is the relaxation of atomic positions around the vacancy. Using ion channeling techniques on NbC _{x} samples Kaufmann and Meyer^{27,28} have concluded that the Nb shell neighboring an isolated C vacancy relaxes outward by 0.11–0.12 Å, about 5% of the Nb-C distance. This result was confirmed by analysis of Debye-Waller factors obtained by x-ray diffraction,²⁹ but elastic diffuse neutron scattering was interpreted in terms of a relaxation of only 0.03 Å (Ref. 26) or 0.05 Å (Ref. 22). Obviously it would be desirable to investigate the effects of such relaxation on the electronic structure in future studies. Kaufmann and Meyer^{27,28} also concluded that the magnitude of the outward relaxation of Nb atoms decreases with increasing va-

cancy concentration, by about 25% at 18% vacancy concentration. This change reflects the strong vacancy-vacancy interaction and supports our suggestion that the XPS peak at -1.9 eV is not representative of an isolated vacancy.

V. SUMMARY

We have applied the muffin-tin Green's function method to calculate the electronic structure of the carbon vacancy in NbC. Unlike previous calculations, this study is both self-consistent and treats the isolated vacancy *in the solid* rather than in a cluster model. A strong vacancy-related resonance of Γ_1 symmetry occurs 2.6 eV below E_F , with a weaker and broader Γ_{15} feature 1.75 eV below E_F . Both arise from the shift of d states on the nearest-neighbor Nb atoms. We suggest that the peak in XPS data on NbC_{0.85} 1.9 eV below E_F represents this Γ_1 symmetry resonance shifted by vacancy-vacancy interactions and relaxation of atomic positions near the vacancy.

Recently Marksteiner *et al.*³⁰ have carried out Korringa-Kohn-Rostoker-CPA calculations on the electronic structure of NbC_{*x*} "alloys." They used nonself-consistent and x -independent potentials determined from overlapping spherical ions placed on a Nb₄C₃ plus vacancy superlattice. In the $x \rightarrow 0$ limit, which is the case we

have considered in this paper, they obtain a vacancy related peak at $E_F - 2$ eV. The peak moves toward E_F with increasing x , lying at about $E_F - 1.1$ eV for $x = 0.85$. This result suggests that most, if not all, of the difference between our value of the binding energy of the peak (2.6 eV) and the experimental value of Höchst *et al.* (1.9 eV) for $x = 0.85$ can be accounted for by the vacancy-vacancy interaction and the lowering of E_F for finite-vacancy concentrations.

The results of this paper can be used as the basis for the calculation of a wide range of properties of NbC_{*x*} in the $x \rightarrow 1$ limit. The defect potential and the crystalline band structure and wave functions are sufficient to give the shift and broadening of the Fermi surface and the residual resistivity. The changes in Fermi surface are believed to be the primary cause of the disappearance of phonon anomalies, which in turn correlate with the sharp drop of superconducting transition temperature with increasing vacancy content.

While the present results clear up the confusion about the electronic spectrum of the carbon vacancy in NbC, other important properties such as the energetics of vacancy formation and migration remain to be answered. These properties represent a more formidable challenge for future studies.

-
- ¹L. E. Toth, *Transition Metal Carbides and Nitrides* (Academic, New York, 1971).
- ²A. L. Gyorgy, S. G. Szklarz, E. K. Harms, A. L. Bowman, and B. T. Matthias, *Phys. Rev.* **125**, 837 (1962); L. C. Toth, M. Ishikawa, and Y. A. Chang, *Acta Metall.* **16**, 1183 (1968).
- ³L. M. Huisman, A. E. Carlsson, C. D. Gelatt, Jr., and H. Ehrenreich, *Phys. Rev. B* **22**, 991 (1980).
- ⁴K. Schwarz and N. Rösch, *J. Phys. C* **9**, L433 (1976).
- ⁵G. Ries and H. Winter, *J. Phys. F* **10**, 1 (1980).
- ⁶H. Höchst, P. Steiner, S. Hüfner, and C. Politis, *Z. Phys. B* **37**, 27 (1980).
- ⁷J. Klima, *J. Phys. C* **12**, 3691 (1979).
- ⁸B. M. Klein, D. A. Papaconstantopoulos, and L. L. Boyer, *Phys. Rev. B* **22**, 1946 (1980).
- ⁹P. Pecheur, G. Toussaint, and E. Kauffer, *Phys. Rev. B* **29**, 6606 (1984).
- ¹⁰W. Kohn and L. J. Sham, *Phys. Rev.* **140A**, 1133 (1965).
- ¹¹L. Hedin and B. I. Lundquist, *J. Phys. C* **4**, 2064 (1971).
- ¹²K. Schwarz, *J. Phys. C* **10**, 195 (1977).
- ¹³R. Podloucky, R. Zeller, and P. H. Dederichs, *Phys. Rev. B* **22**, 5777 (1980).
- ¹⁴P. J. Braspenning, R. Zeller, A. Lodder, and P. H. Dederichs, *Phys. Rev. B* **29**, 703 (1984).
- ¹⁵R. Zeller, J. Deutz, and P. H. Dederichs, *Solid State Commun.* **44**, 993 (1982).
- ¹⁶M. Morinaga, K. Sato, A. Aoki, A. Adachi, and J. Harada, *Philos. Mag. B* **47**, 107 (1983).
- ¹⁷J. H. Weaver and F. A. Schmidt, *Phys. Lett.* **77A**, 73 (1980).
- ¹⁸J. D. Venables and M. H. Meyerhoff, in *Proceedings of the 5th Materials Research Symposium*, (Natl. Bur. Stand. (U.S.) Circ. No. 364, U.S. GPO, Washington, D.C., 1972), p. 583.
- ¹⁹J. Billingham, P. S. Bell, and M. H. Lewis, *Acta Crystallogr. Sect. A* **28**, 602 (1972).
- ²⁰M. Sauvage and E. Parthé, *Acta Crystallogr. Sect. A* **28**, 607 (1972).
- ²¹J. Hauck, *J. Less-Common Met.* **105**, 283 (1985).
- ²²J. P. Landesman, A. N. Christensen, C. H. de Novion, N. Lorenzelli, and P. Convert, *J. Phys. C* **18**, 809 (1985).
- ²³Hj. Matzke, *Solid State Ionics* **12**, 25 (1984).
- ²⁴V. Moisy-Maurice, C. H. de Novion, A. N. Christensen, and W. Just, *Solid State Commun.* **39**, 661 (1981).
- ²⁵R. Kaufmann, G. Linker, and O. Meyer, *Nucl. Instrum. Meth. Phys. Res.* **218**, 647 (1983).
- ²⁶V. Moisy-Maurice, C. H. de Novion, A. N. Christensen, and W. Just, *Solid State Commun.* **39**, 661 (1981).
- ²⁷R. Kaufmann and O. Meyer, *Phys. Rev. B* **28**, 6216 (1983).
- ²⁸R. Kaufmann and O. Meyer, in *Superconductivity in d- and f-Band Metals*, edited by W. Buckel and W. Weber (Kernforschungszentrum Karlsruhe, Karlsruhe, 1982), p. 443.
- ²⁹T. H. Metzger, J. Peis, and R. Kaufmann, *J. Phys. F* **13**, 1103 (1983).
- ³⁰P. Marksteiner, P. Weinberger, A. Neckel, R. Zeller, and P. H. Dederichs, *Phys. Rev. B* **33**, 6709 (1986).